J Therm Anal Calorim (2010) 99:415–421
DOI 10.1007/s10973-009-0461-1

Thermal behaviour of tin(II/IV) phosphates prepared by various methods

L. Szirtes · J. Megyeri · E. Kuzmann

Received: 8 June 2009 / Accepted: 2 September 2009 / Published online: 19 September 2009

Abstract Tin(II/IV) phosphate was prepared by various synthetic methods. The different methods resulted in tin phosphate with different properties, i.e., different crystalline form and behaviour during thermal treatment. The prepared materials have 3 mol water of crystallisation, which they lose in different ways. Total mass loss was between 20 and 30%. This could be connected with water loss, going generally in two steps in parallel with endothermic processes. At the end of thermal treatment, tin pyrophosphate is obtained, irrespective of the method of preparation used.

Keywords Sn(II) · Sn(IV) · Phosphate · Thermal analysis

Introduction

Over the past 20–25 years, the metal phosphates (primarily the tetravalent metal phosphates) have been extensively studied because of their potential use in catalysis, in ion exchange, and in phase separation [1–4]. In this series, the α-tin phosphate has been obtained [5].

Nowadays tin phosphate [6–8] and some of its open-framework derivatives are widely used in catalytic reactions, in thin-film battery production [9, 10], in nuclear waste utilization processes, and in nuclear medicine as oxidising agents [11–19].

L. Szirtes (✉) · J. Megyeri
Institute of Isotopes of the Hungarian Academy of Sciences, P.O. Box 77, 1525 Budapest, Hungary
e-mail: szirtes@iki.kfki.hu

E. Kuzmann
Laboratory of Nuclear Chemistry, CRC of the Hungarian Academy of Sciences at Eötvös University, P.O. Box 32, 1518 Budapest, Hungary

The observation that there is a close relationship between the structure of the end product and the method of synthesis is very important in practical application. It is of the same importance as the relationship between thermal decomposition and compound structure, and the study of the influence of metal and ligand nature on the process of thermal decomposition. Therefore, many authors have investigated these phenomena [20–32].

This study is an effort to investigate the thermal behaviour of tin(II/IV) phosphates prepared in different ways.

Experimental

Synthesis

The typical methods of synthesis were as follows:

(1) 6.77 g $SnCl_2{\cdot}2H_2O$ (Sigma) and 4.1 g $NH_4)_3PO_4{\cdot}5H_2O$(Sigma) were mixed and then transferred to a quartz bottle and heated in an oven, under an argon-gas blanket, at 200 °C for 1 h, then at 300 °C for 1 h, and finally at 400 °C for 2 h. The resulting glassy-type material was ground and stored at room temperature under an argon-gas blanket (Sample 1).

(2) As a first step, 5.46 g $SnCl_2{\cdot}2H_2O$ was dissolved in 20.86 cm^3 HF (40%) solution; the mixture was then diluted to 25 cm^3 with de-ionized water and heated at 80 °C. At this temperature 4.744 g H_3PO_4 (85%) was added to the solution, very slowly, with constant stirring,. The mixture was maintained at 80 °C for 7 days with magnetic stirring. After cooling to room temperature, 20 cm^3 ethanol (in two parts) was added. The resulting precipitate was thoroughly washed with de-ionized water and the dried in desiccators at 60 °C to constant mass (Sample 2).

(3) 852.8 g H_3PO_4 (85%) and 189.3 g conc. HNO_3 were mixed, diluted to 1,000 cm^3 with de-ionized water, and heated at 60 °C. To this solution was added slowly under vigorous stirring 9.54 g $SnCl_2{\cdot}2H_2O$. The stirring was continued until the mixture became homogeneous. The homogeneous solution was maintained at this temperature, under an argon-gas blanket and with constant stirring, for 100 h. The precipitate was then thoroughly washed with de-ionized water until pH ~3.5–4.0 and dried in vacuum desiccators above P_2O_5 (Sample 3).

Chemical composition

The chemical composition of the end products was determined using the method of prompt gamma-activation analysis (PGAA). This method is a rapidly developing nuclear analytical technique. When a nucleus absorbs a neutron, prompt gamma radiation is emitted. This radiation is characteristic, i.e., the gamma-ray energy identifies the element (or even its isotope), and its intensity is proportional to the amount of the element. The mass of the elements can be determined from peak areas by using the detector efficiency and spectroscopic data of the elements [33].

The measurements were performed at the cold-neutron PGAA facility of the Budapest Research Reactor. The neutron flux at the sample position was 1.2×10^{12} cm^{-2} s^{-1}. Irradiation lasted 13–15 h. The temperature was 35 K and the sample masses were about 0.5 g each. The determination limit was 0.05 atom%.

The results are collected in Table 1.

Identification

X-ray analysis

X-ray diffraction (XRD) analysis with Bragg–Brentano geometry, on powder samples previously pressed into the sample holder, was performed with a DRON-2 computer-controlled diffractometer (at 45 kV and 35 mA) with β filtered $Co_{K\alpha}$ radiation ($\lambda = 1.7890$ Å) at 25 ± 1 °C. The goniometer speed was 1/4° min^{-1} in the range $2\Theta =$ 3–110°. When data collection was complete, the first few lines of the pattern were re-measured, to monitor of the stability of the X-ray source. The diffraction patterns were evaluated using "Exray" peak searching software (Z. Klencsár, Personal communication, 1998). During the estimation, the effect of texture on line intensity was taken into consideration.

Table 1 Molar quantity of elements (atom%)

Element	Sample		
	1	2	3
H (1)	62.4	51.0	57.5
F (9)	–	–	–
P (15)	25.0	33.0	28.0
Sn (50)	12.5	16.9	14.7
Total	99.9	100.9	100.2

Mössbauer studies

The Mössbauer spectra of the investigated samples were obtained in transmission geometry, using a ~600 MBq activity $Ba^{119}SnO_3$ (room temperature) source. The patterns were recorded at 298 K. The spectra were fitted using "Mosswinn" refining computer software (Z. Klencsár, Personal communication, 1996).

Thermal analysis

The measurements were carried out using a Mettler-TA1-HT type computer-controlled thermo-balance, which simultaneously provided DTA and TG data. The heating rate was 5 K min^{-1} in the temperature range 290–1,500 K. The reference material was dehydrated Al_2O_3, the atmosphere was air, and a Pt crucible was used. The data obtained were evaluated by use of suitable computer software.

Results and discussion

Comparison of the data in Table 1 reveals the tin/phosphorus ratio was 1:2 for all the samples investigated. The analysis does not show chloride ions in the end materials, and it was found that the chemical composition of samples 1 and 3 was practically are the same.

The patterns of XRD measurements are presented in Fig. 1.

The pattern (Fig. 1a) for the glassy-type material (Sample 1) obtained from the first method of preparation, showed amorphous character. The pattern characteristic of sample 2 (Fig. 1b) showed that this material is highly crystalline. After evaluation and refinements it was found that crystallographically this material is a double-phase system. Its structure is monoclinic of space group $P2_1/n$. On the basis of data from analytical and Mössbauer study the two phases found could be identified, at room temperature, as tin phosphates of composition $Sn(H_2PO_4)_4{\cdot}nH_2O$ and $Sn(HPO_4)_2{\cdot}nH_2O$. The unit cell dimensions are collected (with data for sample 3) in Table 2.

The XRD pattern of sample 3 (Fig. 1c) showed that this material is also highly crystalline. As a result of evaluation

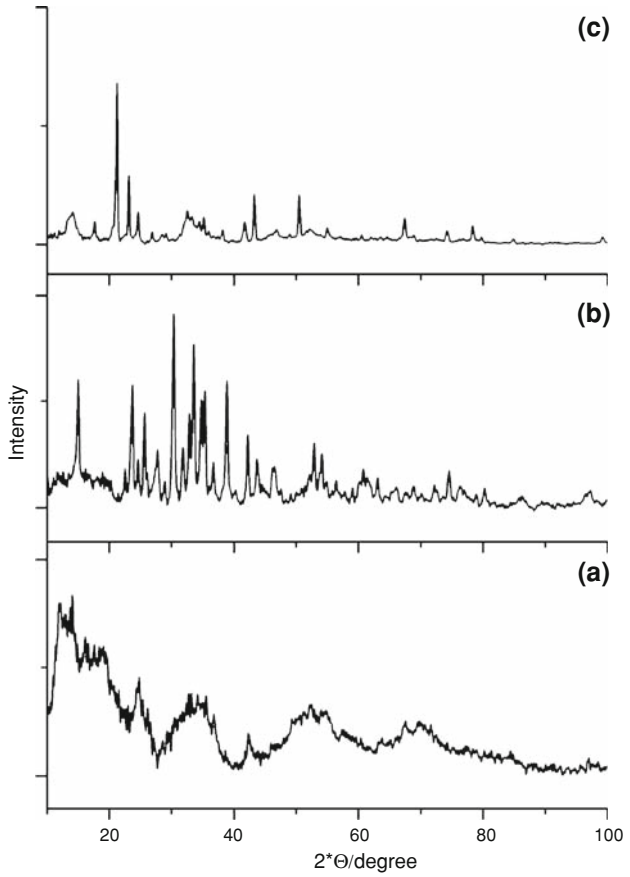

Fig. 1 Fragments of the XRD patterns of the samples investigated: **a**, sample 1; **b**, sample 3; **c**, sample 2

Table 2 Crystal data

	Sample no.		
	2 $Sn(H_2PO_4)_2$	1 $Sn(HPO_4)_2$	3 $Sn(HPO_4)_2$
a (Å)	4.5860(2)	8.6121(2)	8.6059(2)
b (Å)	13.6180(2)	4.9649(2)	4.9596(2)
c (Å)	5.8180(2)	15.8608(3)	15.8613(3)
$\beta°$	99.61(3)	98.87(5)	98.48(5)
V (Å^3)	358.68	669.83	669.51
d_m (g cm^{-1})	3.9801	2.2773	2.1892
d_c (g cm^{-1})	3.9789	2.2767	2.1879
Mass absorption coefficient (cm g^{-1})	0.00	146.41	146.32
Z	7	7	7

and refinement of the pattern the cell dimension obtained were very similar to those obtained for sample 1 (Table 2).

The structures of the different tin phosphates $Sn(H_2PO_4)_2{\cdot}n_1H_2O$ and $Sn(HPO_4)_2{\cdot}n_2H_2O$ consist of sheets. The SnO_3 trigonal-pyramids and the PO_4 tetrahedra connect together to form infinite two dimensional sheets. In this configuration, each tin atom coordinates three phosphate groups. The O–O distance in the sheets was ~2 Å, which is the average for hydrogen-bonded phosphate groups. Comparison of these data with those for mono and dihydrate phosphate revealed some distortion in the structure of the latter compound.

The Mössbauer pattern of first sample (Fig. 2a) contains a singlet with isomer shift of 0.04 mm/s, which is characteristic of tin(IV). The broadening of the singlet can be mainly attributed to the amorphous character of the sample. In case of second sample, the pattern recorded at 298 K (Fig. 2b), contains three peaks which can be decomposed to one singlet and two quadruple doublets, characteristic of tin(II). The weak singlet is characteristic of tin(IV) whereas the doublets show the tin(II) species. From the spectra it is readily apparent that this material predominantly contained tin in oxidation state 2. The pattern recorded for the third sample (Fig. 2c), showed an asymmetric peak which contained only one singlet with an isomer shift of $\delta = 0.01$ mm s^{-1}, but ~1% of the tin(II) doublet can also be observed. This singlet is characteristic of tin(IV); i.e., this material mostly contains tin in oxidation state 4.

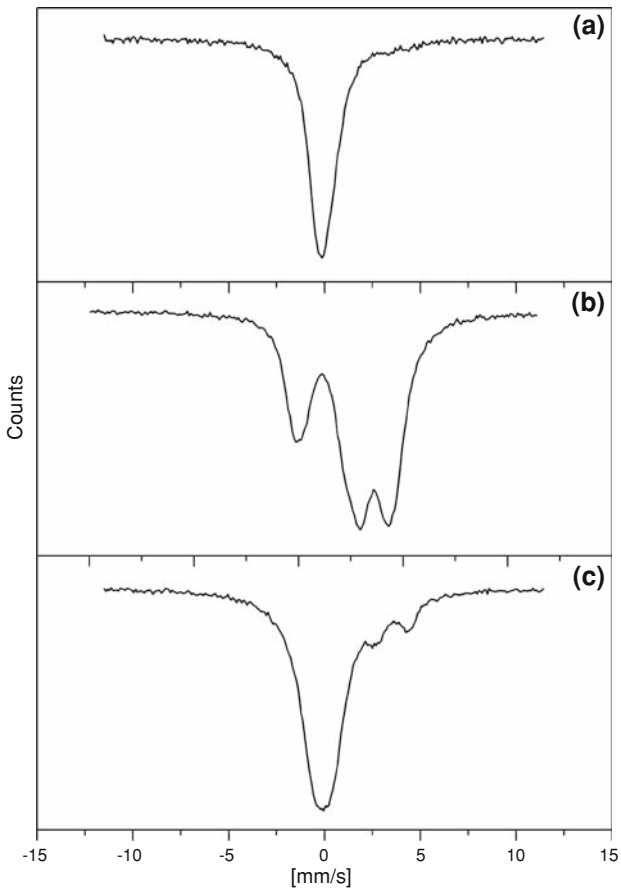

Fig. 2 Patterns from Mössbauer study of the samples investigated: **a**, sample 1; **b**, sample 2; **c**, sample 3

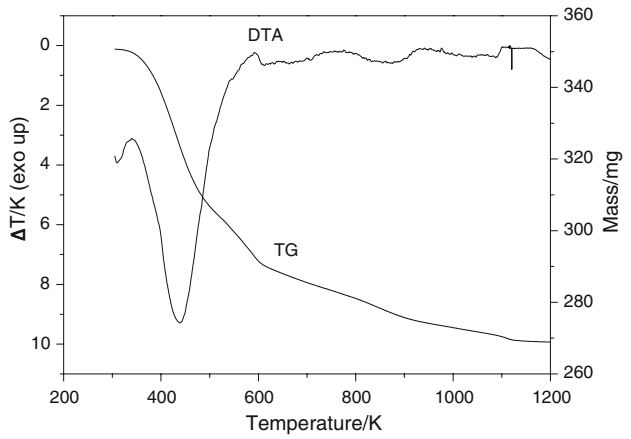

Fig. 3 The DTA–TG curves for sample 1

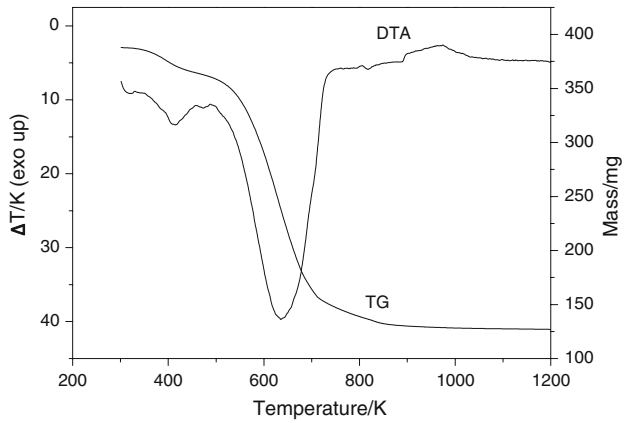

Fig. 4 The DTA–TG curves for sample 3

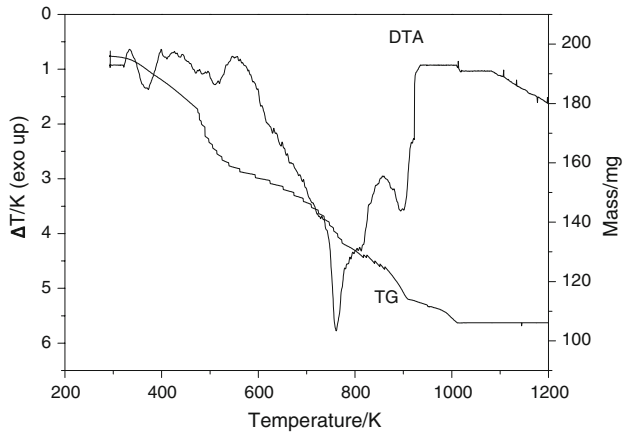

Fig. 5 The DTA–TG curves for sample 2

Data from thermal analysis are shown in Figs. 3, 4 and 5, respectively, and collected in Table 3.

The vitreous glassy-type material (sample 1) of composition $Sn(HPO_4)_2{\cdot}nH_2O$ decomposed during thermal treatment. The decomposition went through two endothermic processes, with mass losses. Taking molecular composition into consideration, these mass losses can be associated with water loss. The first endothermic process occurs in the temperature range 298–535 K, with a peak at 450 K; the mass loss of 18.87% can be attributed to loss of water of crystallisation. The next endothermic process, occurring in two steps in the temperature ranges 625–760 K and 760–1,100 K, with peaks at 675 and 875 K, respectively, can be attributed to loss of structural water. This water originated from chemical decomposition of phosphate groups. In parallel with these processes, a continuous loss of mass resulted in a decrease of 7.87%. In our experience this process occurs much more slowly in the presence of Sn(IV) than in the presence of Zr(IV) or Ti(IV), etc.

As a result of these processes, the total mass lost by the material was 26.74%. In addition to the processes described, an exothermic process was observed in the temperature range 1,130–1,140 K. This process, without mass loss, covered the crystalline phase transition of SnP_2O_7 from monoclinic to orthorhombic. The latter data correlate quite well with literature data given by Van Weser [34]. On the basis of the DTA–TG curves in Fig. 3, the following scheme can be proposed for thermal decomposition of this material:

$$Sn(HPO_4)_2{\cdot}3H_2O \xrightarrow{-3H_2O} Sn(HPO_4)_2 \xrightarrow{-H_2O} SnP_2O_7 \xrightarrow{\text{Phase trans.}} SnP_2O_7.$$

By comparing the chemical composition data and the DTA–TG curves, the amounts of the two different types of water lost were calculated. The result was three moles water of crystallisation lost and one mole structural water lost per molecule unit.

The end product of preparation, denoted "3" (sample 3), with the same composition, $Sn(HPO_4)_2{\cdot}nH_2O$, also decomposed in a few steps during thermal treatment. The processes in this case were similar, but not quite the same as those described above. The main difference was in the mode of loss of water of crystallisation, i.e., the total quantity of three moles of such water lost per molecule unit in two steps. The first loss, in the temperature range 298–520 K (with a peak at 460 K), was 8.32% of the original mass; the next loss, in the temperature range 520–850 K (with a peak at 610 K) was 16.91%. Together, these processes resulted a total mass loss of 25.23%. Comparison of the data for chemical composition and DTA–TG curves, for the first process the loss was calculated to be one mole of water loss; for the second process three moles of water were lost per molecule unit. On the basis of molecule composition, the latter process must cover one mole of

Table 3 Thermal analytical data

Sample	Process	Temp. range/K	Peak temp./K	Mass loss/%		Mole water of crystallisation
				Partial	Total	
1	Endo	298–525	450	18.87	26.74	3
	Endo	625–760	675			
	Endo	760–1,100	875	7.87		
	Exo	1,130–1,140		w.m.l.		
2	Endo	298–415	360	1.16	29.51	0.5 + 2.5
	Endo	415–571	480	11.26		
	Endo	570–860	680	12.82		
	Endo	860–960	890	4.27		
	Exo	1,100		w.m.l.		
3	Endo	298–520	460	8.32	25.23	3
	Endo	520–850	610	16.91		
	Exo	870–1,030	960	w.m.l.		

w.m.l. = without mass loss

structural water, originating from dehydration of phosphate groups, and the other two moles of water must be water of crystallisation. It is possible that two differently bonded types of water of crystallisation exist in the highly crystalline material, i.e., one mole is bonded weakly to the surface of the crystals and the other two moles are accommodated between the layers and bonded much more strongly and, as a result, lost at a higher temperature.

At temperatures between 870 and 1,030 K an exothermic process was observed without mass loss. This is, perhaps, connected with the same crystalline phase transition of pyrophosphate groups as mentioned above. A difference in the speed of this process was observed in comparison with that of the glassy-type material.

On the basis of the DTA–TG curves in Fig. 4, the following scheme can be proposed for thermal decomposition of this material:

$$\mathrm{Sn(HPO_4)_2{\cdot}3H_2O} \xrightarrow{-\mathrm{H_2O}} \mathrm{SnHPO_4)_2 \cdot 2H_2O}$$

$$\xrightarrow{-(2+1)\mathrm{H_2O}} \mathrm{SnP_2O_7} \xrightarrow{\text{Phase trans.}} \mathrm{SnP_2O_7}$$

For sample 2 (Fig. 5) the situation was more complicated. It is apparent from the Mössbauer study that this material contains tin atoms in both the two ($\sim$90%) and four ($\sim$10%) oxidation states. Comparing these data with those from chemical analysis, we assumed the end product of the method of preparation, denoted "2" (sample 2), consisted of tin phosphate of different compositions. On the basis of the data given above, these are $Sn(H_2PO_4)_2{\cdot}n_1H_2O$ and $Sn(HPO_4)_2{\cdot}n_2H_2O$.

The DTA–TG curves of the sample are shown in Fig. 5. The DTA curve contains four endothermic processes occurring with mass loss and an exothermic process without mass loss. The first endothermic process occurs in the temperature range 298–415 K, with a peak at 360 K. The second occurs at 415–571 K with a peak at 480 K. These processes together resulted in 12.42% mass loss, divided between them as 1.16 and 11.25%, respectively. The third endothermic process was observed in the temperature range 570–860 K, with a peak at 680 K, and the last in the range 860–960 K, with a peak at 890 K. These processes together resulted in 17.09% mass loss, divided between them as 12.82 and 4.27%, respectively. Finally, an exothermic process without mass loss was observed at 1,100 K. Consequently, after completion of the thermal treatment the total mass loss of the sample was 29.51% of the original mass.

On the basis of the original molecular composition, the endothermic processes with mass loss were identified as water loss, and knowing the TG data it was possible to calculate their quantity. On the basis of literature data [4] and our earlier experience, such phosphate type materials consist of water of crystallisation and structural water, the latter originating during dehydration of phosphate groups. On the basis of this knowledge, the first and second processes were identified as loss of water of crystallisation whereas the third and fourth were identified as loss of structural water. From the DTA–TG data, loss of 2.5 + 0.5 moles of water of crystallisation and 2 + 1 moles of structural water, per molecule unit, from the original molecular composition were calculated.

As can be seen from the DTA curve, the part of the material containing tin in oxidation state four loses its water of crystallisation faster, at relatively lower temperature, than those parts with tin in oxidation state two. The opposite was observed for structural water loss. We believe

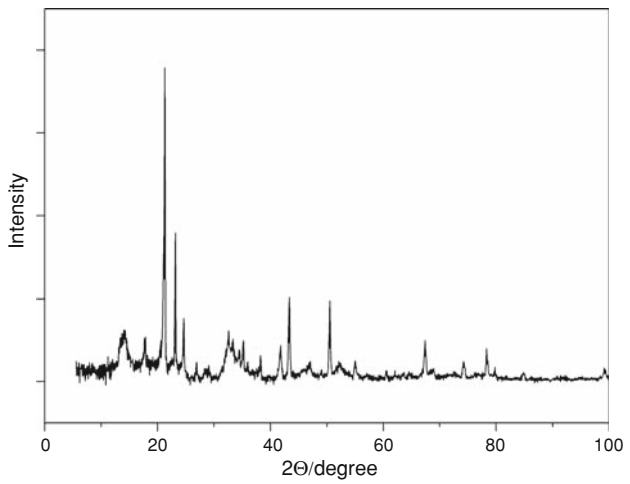

Fig. 6 A fragment of the XRD pattern of SnP_2O_7

the phenomena observed can be explained on the basis of the different compositions and the different structure arising from them.

Finally, the exothermic process observed can be connected with the crystalline phase transition of SnP_2O_7 (end product of thermal treatment) from monoclinic to orthorhombic, which occurs at approximately 1,100 K.

On the basis of these results, the following scheme can be proposed for thermal decomposition of this material:

$$\mathrm{Sn\ (H_2PO_4)_2{\cdot}2.5H_2O} \xrightarrow{-2.5\mathrm{H_2O}} \mathrm{Sn\ (H_2PO_4)_2} \xrightarrow{-2\mathrm{H_2O}}$$

$$\mathrm{SnO \cdot SnP_2O_5} \xrightarrow{\text{Phase trans.}} \mathrm{SnP_2O_5}$$

$$\mathrm{Sn(HPO_4)_2{\cdot}0.5H_2O} \xrightarrow{-0.5\mathrm{H_2O}} \mathrm{Sn(HPO_4)_2} \xrightarrow{-\mathrm{H_2O}}$$

$$\mathrm{SnP_2O_7} \xrightarrow{\text{Phase trans.}} \mathrm{SnP_2O_7}.$$

To verify this assumption, the end product obtained after completion of the thermal treatment was studied by XRD. The XRD pattern of this material is shown in Fig. 6.

Both this evaluation and comparison with the appropriate ASTM card (no. 75–1143) unequivocally confirm the presence of tin pyrophosphate.

Conclusions

The different methods of preparation result tin phosphate of different quality. The first method results in a vitreous, glassy-type material with a crystallographically amorphous state. In this material, the tin atoms are in oxidation state four.

The third method of preparation results in the same tin phosphate but in a highly crystalline form. During thermal treatment, however, these materials behaved differently. Whereas for the first sample loss of water of crystallisation occurs in one step, in a relatively narrow temperature range, for the second sample the same water is lost in two parts. This must mean the water of crystallisation is bonded differently in the latter form; i.e., the smaller part weakly, perhaps on the surface of the molecule whereas the other two thirds is present between the layers, and is strongly bound. This explains the loss of this part of the water at a higher temperature, together with the structural water.

The second method of preparation also results in highly crystalline material. This tin phosphate contains approximately 90% of the tin atoms in oxidation state two and its properties were slightly different from those of the other two samples investigated. The tin atoms with different oxidation state in this material result in different phosphate composition. The tin phosphates of different compositions lost their water of crystallisation and structural water together in relatively narrow temperature ranges.

In general, all the samples investigated behave similarly, but not exactly identically, during thermal decomposition. Irrespective of the method of preparation, they have three moles of water of crystallisation per molecule unit, which are lost differently, and at the end of thermal treatment the tin pyrophosphate is the result.

Acknowledgements The authors are grateful to Zs. Révay for performing the prompt gamma-activation analysis.

References

1. Harrison FG. The structural chemistry of bivalent Ge, Sn and Pb. Coord Chem Rev. 1976;20:1–36. (and references therein).
2. Polarz S, Smarsky B. Nanoporous materials. J Nanosci Technol. 2002;2/6:581–612. (and references therein).
3. Cheetham AK, Férey G, Loiseau T. Hybrid inorganic–organic materials and their application. Angew Chem Int Ed. 1999;38:3268–92.
4. Clearfield A, editor. Inorganic ion exchange materials, other group (IV) acid salts (Chap. 2). Boca Raton, FL: CRC Press; 1982.
5. Weiss MA, Michel E. Kationenaustausch und eindimensionales innerkristallines Quellungsvermögen bei den isotypen Verbindungen $H_2[M(XO_4)_2]{\cdot}H_2O$; (X = P, As; M = Ti, Zr, Sn). Z Naturforsch. 1967;B22:1100–12.
6. Winkler VA, Thilo E. Über eine reiche saurer Verbindungen $HX^{V}P_2O_8$ und $H_2X^{IV}P_2O_8$ mit schichtstrur. Z Anorg Allg Chem. 1966;346:92–112.
7. Costantino U, Gasperoni A. Crystalline insoluble acid salts of tetravalent metals XI. J Chromatogr. 1970;51:289–96.
8. Berezovska IS, Yanishpolskii VV, Tartykh VA. Synthesis of mesoporous silicas inside large pores of inorganic matrix. J Therm Anal Calorim. 2008;94(3):649–53.
9. Yang K, Li DH, Chen S, Wu F. Thermal behaviour of Nickel/metal hybrid battery during charging and discharging. J Therm Anal Calorim. 2009;95(2):453–9.
10. Takei T, Yonesaki Y, Kumada N, Kiomura N. Preparation of oriented titanium phosphate and tin phosphate/polyaniline electrochemical deposition. Langmuir. 2008;24(16):8554–60.

11. Stenina A, Aliev AD, Glukhov IV, Spiridonov FM, Yaroslavtsev AB. Cation mobility and ion exchange in acid tin phosphate. Solid State Ionics. 2003;162–163:191–5.
12. Fuller MJ. Ion exchange properties of tin (IV) materials-IV. J Inorg Nucl Chem. 1971;33:559–66.
13. Ho WH, Yen SK. Electrochemical synthesis of SnHPO4/H3PO3 on Pt and forming SnP_2O_7. Electrochem Solid State Lett. 2005;8:C134–7. and references therein.
14. McDonald RC, Hau HH, Eriks K. Crystallographic studies of tin (II) compounds 1. Inorg Chem. 1976;15:762–5.
15. McDonalds RC, Eriks K. Crystallographic studies of tin (II) compounds 2. Inorg Chem. 1980;19:1237–41.
16. Natarajan S, Easwaramoorthy M, Cheetham AK, Rao CNR, A three-dimensional open-framework tin (II) phosphate exhibiting reversible dehydration and ion exchange properties, Chem Commun. 1998; 1561–2.
17. Salami TO, Marouchin K, Zavalij PY, Scott, Oliver RJ. Three low-dimensional tin oxalate and tin phosphate materials: BING-4, -7, and -8. Chem Mater. 2002;14(11):4851–7.
18. Gon-Lee J, Son D, Kim C, Park B. Electrochemical properties of tin phosphates with various mesopore ratios. J Power Sources. 2007;172:908–12.
19. Schütz C, Dwars T, Schnorpfeil C, Radnik J, Menzel M, Kragl U. Selective polymerization of propylene oxide by a tin phosphate coordination polymer. J Polym Sci A. 2008;45(14):3032–41.
20. Jiang T, Lough A, Ozin GA. Room temperature self-assembly of $(DABCOH)_2Sn_3S_7$. Adv Mater. 1998;10:42–6.
21. Natarajan S, Attfield MP, Cheetham AK. $[H_3N(CH_2)_2NH_3]_{0.5}[Sn_4P_3O_{12}]$: an open-framework tin(II) phosphate. Angew Chem Int Ed Engl. 1997;36:978–80.
22. Francis MD, Tofe AJ, Hiles RA, Birch CG, Beven JA, Grabenstetter RJ. Inorganic tin: chemistry, disposition and role in nuclear medicine. Int J Nucl Med Biol. 1981;8:145–52. (and references therein).
23. Noronha OPD. Time-dependent characteristic s of Sn-complexes for preparing ^{99m}Tc labelled radiopharmaceuticals and their bioavailabilities. Nucl Med. 1978;17(3):110–25. (and references therein).
24. Mathew M, Schroeder LW, Jordan TH. The crystal structure of anhydrous stannous phosphate, $Sn_3(PO_4)_2$. Acta Cryst. 1977; B33:1812–6.
25. Jordan TH, Schroeder LW, Dickens B, Brown WE. Crystal structure of stannous hydroxide phosphate. Inorg Chem. 1976;15/8:1810–4.
26. Natarajan S. Synthesis and structural characterisation of a novel tin (II) oxyphosphate. J Mater Chem. 1998;8:2757–60.
27. Varshney KG, Rafiquee MZA, Somya A. Synthesis, characterisation and adsorption behaviour of TX-100 based Sn (IV) phosphate, a new hybrid ion exchanger. J Therm Anal Calorim. 2007;90(3):663–7.
28. Alberti G, Torracca E, Conte A. Stoichiometry of ion exchange materials containing zirconium and phosphate. J Inorg Nucl Chem. 1966;28:607–12.
29. Varshney KG, Jain V, Agrawal A, Mojumdar SC. Pyridine based Zr (IV) and Sn (IV) phosphates as new and novel intercalated ion exchangers. J Therm Anal Calorim. 2006;86(3):609–21.
30. Crespi MS, Zorel HE Jr, Ribeiro CA. Thermal behaviour of the Ti(IV), Zr (IV), and Pb(II) complexes with 5-nitro-8-hydroxyquinoline. J Therm Anal Calorim. 2003;72:507–14.
31. Surenda Nath KV, Tandon SN. Synthesis and characterisation of a new crystalline tin (II) arsenophosphate ion exchanger. Can J Chem. 1990;68:346–9.
32. Pozas-Tormo R, Moreno-Real L, Martinez-Lara M, Rodrigez-Castellon E. Ion exchange reactions of n-butylamine intercalates of tin (IV) hydrogen phosphate and hydrogen uranyl phosphate with Co (III) complexes. Can J Chem. 1986;64:35–9.
33. Molnár GL, editor. Prompt gamma activation analysis with neutron beams. Dordrecht: Kluwer; 2004.
34. Van Weser JR. Phosphorus and its compounds, vol. I. NY: Interscience Co; 1958.